A Multiclass, Multiproduct Covid-19 Convalescent Plasma Donor Equilibrium Model

Anna Nagurney
Department of Operations and Information Management
Isenberg School of Management
University of Massachusetts
Amherst, Massachusetts 01003

Pritha Dutta*
Department of Management and Management Science
Lubin School of Business
Pace University
New York, New York 10038

May 2020

Abstract: In this paper, we develop a multiclass, multiproduct equilibrium model for convalescent plasma donations in the Covid-19 pandemic. The potential donors are situated at different locations and the donor population at each location can be separated into different classes based on their motivation and the product for which they provide donations at a collection site. The model captures the competition between nonprofit and for profit organizations seeking convalescent plasma donations, which is a characteristic of this new market. A variational inequality formulation of the equilibrium conditions and qualitative properties of the model are provided. We also present a capacitated version of the model. Numerical examples of increasing complexity are presented and solved using the modified projection method. The results reveal multiclass, multiproduct donor behavior under different scenarios which can inform policy makers during this pandemic and beyond.

Keywords: convalescent plasma, pandemic, Covid-19, blood donations, networks

* corresponding author; email: pdutta@pace.edu

1. Introduction

The Covid-19 pandemic has disrupted the globe, severely compromising economic, educational, and social activities as well as healthcare. The uncertainty surrounding a vaccine and timeline, coupled with, at present, no cure, and the pain, suffering, and attributable deaths of almost three hundred thousand, with millions infected, as of May 14, 2020 (Our World in Data (2020)), are calling for innovative treatments.

One treatment that appears to be especially promising is that of convalescent plasma (Bloch et al. (2020), Casadevall and Pirofski (2020), Duan et al. (2020), Shen et al. (2020)). Such convalescent plasma is the plasma or liquid part of blood obtained from recovered Covid-19 patients which contains antibodies that can fight the virus SARS-CoV-2 causing the disease (Hererra (2020)). According to a recent study on 39 Covid-19 patients, researchers at Mount Sinai Medical Center in New York found a trend towards better survival rates for patients who received convalescent plasma (Beasley (2020)). As more Covid-19 patients recover from the coronavirus, which originated in Wuhan, China, the supply of convalescent plasma from willing donors increases.

Although the full effects of the use of convalescent plasma as therapy on Covid-19 patients is still undergoing clinical trials and investigation, convalescent plasma therapy has been used to treat other infectious diseases in the past (Ferguson et al. (2020)). Several studies have been carried out to test the effectiveness of convalescent plasma treatment in the case of the Ebola virus infection (Winkler and Koepsell (2015), Van Griensven et al. (2016)). Mair-Jenkins et al. (2015) conducted an exploratory meta-analysis that showed the positive effects of using convalescent plasma for the treatment of severe acute viral respiratory infections, including those caused by related coronaviruses (SARS-CoV and MERS-CoV).

Given the potential of convalescent plasma serum to act as a cure for the pandemic, the United States Food and Drug Administration (FDA), in partnership with academics and industry, has begun a nation-wide effort to facilitate the development of two investigational therapies: one on convalescent plasma treatment and the other on hyperimmune globulin (Sheridan (2020)). Hyperimmune globulin is a concentrated antibody serum derived from plasma that can possibly prevent or terminate infection in the future (Aleccia (2020)). According to Aleccia (2020), there also exists a possible third treatment, monoclonal antibody therapy. This therapy uses antibody-producing cells from high-antibody donors to produce lab-produced molecules to battle Covid-19.

There has also been increasing focus globally on convalescent plasma therapy in treating Covid-19 patients, with clinical trials for this investigational therapy approved in several

parts of the world. The European Commission, jointly with the European Blood Alliance (EBA), the European Center for Disease Prevention and Control (ECDC), and health care professionals is driving the study on convalescent plasma treatment in Europe. EBA is emphasizing data reporting and information sharing among blood banks and clinicians through an open database that they are developing to ensure immediate availability of critical information on donor selection, plasma collection processes, etc. (EBA 2020)). At the beginning of May 2020, the National Ethics Committee in India also approved the Indian Council of Medical Research's (ICMR) request to conduct clinical trials in 21 hospitals across the country to study the effectiveness of convalescent plasma treatment (MD Bureau (2020)).

In the United States, researchers, physicians, nonprofit organization such as blood banks, hospitals, the Mayo Clinic, and government regulatory bodies have come together to investigate the merits of this therapy. In order to drive collections they are trying to raise awareness about convalescent plasma treatment among recovered individuals through announcements on their websites and initiatives such as the National Covid-19 Convalescent Plasma Project. Earlier in April 2020, the FDA launched a website to guide recovered Covid-19 patients to plasma collection centers and issued guidelines for plasma collection by nonprofit blood banks such as the American Red Cross, the New York Blood Center, as well as hospitals, for treating severely ill patients (Food and Drug Administration (2020a)). The American Red Cross is collecting convalescent plasma at over 170 locations across the country (Davies (2020)).

According to FDA's latest guidelines (Food and Drug Administration (2020b)), individuals who have fully recovered from Covid-19 and have shown no symptoms for at least two weeks prior to donation are eligible to donate plasma. The donors must have had a prior diagnosis of Covid-19 documented by a laboratory test. In addition, they must meet the regular donor criteria of age and weight and have passed a medical history screening in order to maintain public health safety. Eligible donors can give convalescent plasma every 28 days (American Red Cross (2020)). Nevertheless, even with the growing number of recovered patients, the donor pool for convalescent plasma is limited. The plasma collection process involves drawing blood from one arm of the donor and sending it through a high-tech machine. The machine collects the plasma separating it from whole blood and then safely returns the red cells back to the donor. According to the Blood Bank of Delmarva the apheresis process takes 45-50 minutes. However, the total visit time including medical screening is over around 75 minutes. After collection, similar to Fresh Frozen Plasma (FFP), convalescent plasma should be frozen within 8 hours and stored at -18C or colder. The manufacturing process for Covid-19 convalescent plasma also includes putting the expiration date of one year from the date of collection on the label (FDA (2020b)). However, once thawed, plasma must be

transfused within 5 days.

While nonprofit blood banks and hospital blood programs have been seeking convalescent plasma for clinical trials conducted by research groups and for treatment of severely ill patients, profit-making companies have also started collecting this potentially life-saving product for supplying blood samples to laboratories and test manufacturers with monetary compensations (Bradley (2020), Life Serve Blood Center (2020)). Profit-making companies typically offer $50 to donors for Covid-19 plasma donations. However, the Takeda Pharmaceuticals' BioLife Plasma Services Center, which is part of an industry producing plasma protein therapies crucial for treating certain rare chronic conditions, has reportedly provided gift cards worth $800 to a couple for making two donations (Aleccia (2020)). In times of crisis such as this it is natural for many people to act altruistically to help the community. For example, in the aftermath of 9/11 there was a surge of blood donations, especially from first time donors which eventually led to wastage of collected blood (Korcok (2002)). However, in the current pandemic scenario, donors may not only derive satisfaction or utility from their altruistic behavior but also receive monetary benefits if they choose to donate to a profit-making company such as Cantor BioConnect, which sells the plasma at high prices to laboratories and test manufacturers even overseas (Bradley (2020)).

It is evident from the above discussion that an interesting market for convalescent plasma, which can be used to treat patients and to develop products such as hyperimmune globulin and other critical therapies, has emerged. This market involves multiple players with different objectives and a limited donor pool. Donors, hence, have several options for donation in terms of the product and the organization. In some cases, individuals who are not eligible to donate plasma for direct treatment due to safety concerns, such as Hasidic women who have recovered from Covid-19, can still choose to donate for hyperimmune globulin creation (Aleccia (2020)). Donors are able to distinguish among the competing organizations collecting convalescent plasma based on their purpose and also the product and its use as well as their own conditions to meet the eligibility criteria for donation for a particular product.

Several studies across different disciplines, including economics, psychology, medicine, and operations research (Andreoni (1990), Gillespie and Hillyer (2002), Evans and Ferguson (2013), Craig et al. (2017), Nagurney and Dutta (2019a)), have been conducted in order to better understand the motivation behind blood donations. In their paper, Evans and Ferguson (2013) reported on a psychometric assessment of altruism that can inform and guide donor recruitment strategies. They used five theoretical dimensions of altruism; namely, impure altruism, kinship, self-regarding motives, reluctant altruism, and egalitarian warm glow to differentiate between donors and non-donors. Their findings suggest that pure altruism

is often not the sole motivation for voluntary blood donors, and that blood donor behavior is rather complex. Based on this analysis, we can assume that the blood or, in this case, the convalescent plasma donor population is not homogeneous and can be separated into several classes on the basis of their motivation as well as appropriate fit for a specific product.

In this paper, we develop a novel multiclass, multiproduct donor model for convalescent plasma which is currently one of the most crucial components in the healthcare system during the Covid-19 pandemic. The model is an equilibrium model and consists of different classes of recovered Covid-19 survivors who meet the criteria for donating convalescent plasma for one or more of the plasma products. The donors are located at origin locations whereas the plasma collection sites are located at destination locations. Each class of donor at an origin location has an associated utility function of donating the plasma for a particular purpose/product at a collection site. There is also a generalized cost, which includes, time, money, potential risk, etc., of going from the origin location to each collection site for a class of donor at an origin. We assume a fixed population of recovered donors of each class at each origin location. The donors reflect their preferences through their utility functions.

We now provide a discussion of the existing literature of relevance to our contributions in this paper. We do emphasize that the topic under consideration in this paper is especially timely and novel as the events surrounding the Covid-19 pandemic rapidly evolve. Furthermore, the unusual market for convalescent plasma with both nonprofits and for profit organizations involved in competing for the plasma in the blood of recovered is quite special and merits investigation.

2. Literature Review

We begin the discussion in this section by highlighting extant literature on the modeling of charitable donations, donor behavior, and preferences. Toyasaki and Wakolbinger (2011) compared two common fundraising techniques using optimization models: fundraising with the option of earmarking donations and fundraising without an earmarking option. They modeled the donor's behavior as well as the relief agency's behavior to analyze the effect of earmarking donations on fundraising costs. Saxton and Zhuang (2013) proposed a game theory model that showed that the amount of charitable contributions made by donors is positively dependent on the amount of disclosure by the nongovernmental organizations (NGOs). The authors distinguish between two core donor preferences: the desire for impact and the desire for publicity, with donors choosing between organizations based on how well the organization satisfies these preferences. Zhuang, Saxton, and Wu (2014) further showed that the disclosure of financial, performance, donor-relations, and fundraising information

is an important tool for nonprofit organizations to attract greater donations as it boosts accountability and public trust. Game theory has also been used to investigate other types of charitable donations such as organ donations (Kessler and Roth (2012)).

There exists a rich body of literature on game theory and equilibrium models developed for humanitarian and public policy issues that have significant societal impact (cf. Muggy and Stamm (2014) and the references therein). Nagurney (1989) and Nagurney (1990) studied human migration with multiclass equilibrium models. Nagurney, Pan, and Zhao (1992a, 1992b), subsequently, expanded the work in this area and developed multiclass human migration models with movement/migration costs and class transformation. Causa, Jadamba, and Raciti (2017) also built on the model of Nagurney (1990) to incorporate uncertainty in the utility functions, the migration cost functions, and the populations. More recently, Nagurney and Daniele (2020) developed a network model with regulations for international human migration problems. Their analysis provides insights on the effects of regulations on the utilities of different classes of migrants. On the other hand, Nagurney, Besik, and Dong (2019) looked at regulations pertaining to world trade policies such as ad valorem tariffs and strict quotas. They developed a spatial price network equilibrium model and analyzed it through numerical examples that reveal important information on the impact of different types of quotas on the utilities of producers and consumer prices.

Nagurney, Salarpour, and Daniele (2019) constructed a Generalized Nash Equilibrium (GNE) model to capture the competition among humanitarian organizations in providing disaster relief along with their budget, capacity, and demand constraints. Nagurney et al. (2018) also studied the competition among humanitarian organizations in post-disaster relief for financial funds based on the initial work by Nagurney, Alvarez Flores, and Soylu (2016). Further extensions were constructed by Nagurney, Salarpour, and Nagurney (2020) in the form of a stochastic game theory model for disaster relief that integrated financial and logistical aspects associated with humanitarian operations, and captured the competitive nature of nonprofits for financial donations as well as for freight service provision. The GNE concept was also utilized therein, along with a variational inequality formulation.

In the domain of the blood supply chain literature, of specific relevance to this paper, Dutta and Nagurney (2019) developed a multitiered integrated blood supply chain competition model with different stakeholders; namely, blood banks, hospitals, and patient payer groups such as Medicare, Medicaid, private insurance companies, etc. The model is based on a blood product pricing scheme aimed at ensuring the economic sustainability of the blood banking industry which is essential for maintaining a steady supply of safe blood in the country. The results of their analysis reveal the benefit of a cost-based pricing scheme

for blood products that takes into account the volume of blood transfused and the actual costs of all the supply chain operations can inform policymakers.

While financial stress on blood banks due to increased competition, reduced demand, and cost-intensive testing operations has been a concern in the blood banking industry in recent times, the challenges associated with blood supply chain management are vast and varied. For a broad literature review on this topic see Nagurney and Dutta (2019b) and Dutta and Nagurney (2019). In this paper, we mention a few recent works on this topic. Piraban, Guerreroa, and Labadie (2019) provide an up-to-date literature review on blood supply chain management. Osorio et al. (2017) use discrete-event simulation to capture flows through the blood supply chain consisting of collection, production, storing, and distribution and an integer linear optimization model running over a rolling horizon to decide the required number of donors, collection methods, and production planning. As the authors point out in their paper, blood supply chain research often deals with specific stages of the supply process. There are few works that integrate all the operations comprising the supply chain (cf. Masoumi, Yu and Nagurney (2017)). Given the life-saving properties of blood products there has been a growing emphasis on research focusing on designing robust blood supply chains in the case of emergencies and disasters (Fazli-Khalaf, Khalilpourazari, and Mohammadi (2019), Khalilpourazari and Khamseh (2019), Samani, Torabi, and Hosseini-Motlagh (2019), and Salehi, Mahtoochi, and Husseini (2019)).

While the above mentioned studies tackle interesting and significant issues, there is a clear dearth of modeling research on blood donor behavior which is a critical and unique part of supply chain management of this life-saving product, which cannot be produced but must be donated. Hosseini-Motlagh, Samani, and Cheraghi (2020) developed a novel mixed possibilistic-stochastic flexible robust model that takes into consideration the critical role played by blood donors. That study included motivational initiatives aimed at encouraging blood donors for maintaining a sufficient blood supply. The authors incorporate factors such as advertisement, education, and medical credits in constructing the motivational function.

There has been extensive research on blood donor recruitment and retention drawing from theories in social and behavioral sciences (Ferguson et al. (2007)). Much of that research is empirical work (Gillespie and Hillyer (2002), Schlumpf et al. (2008), Schreiber et al. (2006)). While the theoretical framework of blood donation focuses on altruism (Andreoni (1990)) as the driving force behind blood donations, there have been studies that investigate other potential sources of motivation. Lacetera, Macis, and Slonim (2013) discussed the effect of rewards and incentives on blood donations to mitigate shortages. Nagurney and Dutta (2019a) modeled the competition among blood banks for donations from voluntary

donors using the level of service quality provided at the blood collection sites as factors driving donations. In this paper, we advance the work on the modeling of donor behavior, specifically, in the case of convalescent plasma in relation to the Covid-19 pandemic, which has unique features, including nonprofit as well as for profit organizations collecting the plasma.

We would also like to mention research pertaining to the Covid-19 pandemic. In Kaplan (2020), the author presents probability models that are used to assess the effectiveness of two policies adopted by countries to contain the outbreak of the infectious disease; namely, case isolation and quarantine within a community during the initial phase of outbreak. Baveja, Kapoor, and Melamed (2020) propose a plan with four strategies to be implemented over a period of 90 days in order to stop the spread of the infectious disease while mitigating its economic repercussions: (a) stop all international, domestic passenger air and intercity bus/train travel; (b) create administrative zones of about 1 million people; (c) stop all non-emergency cross-zonal travel except for transportation of goods, and (d) deploy an information-driven service value chain to control the spread of the pandemic within a zone. In another recent publication, Ivanov (2020) develops a new concept of Viable Supply Chain (VSC) drawing from the principles of agility, resilience, and sustainability. The author mentions that the VSC model can help firms make decisions on recovery and re-building of their supply chains in the aftermath of a global crisis such as the Covid-19 pandemic. Rassia (2020) presents an interesting perspective on the need to focus on human values and human interaction with nature in case of architectural designs to create safe spaces protecting people in conditions of crisis. The Covid-19 outbreak is a good example to study since the best way to avoid the infection is to stay indoors; specifically, at home.

The remainder of the paper is organized as follows. In Section 3, we construct the multi-class, multiproduct convalescent plasma donor model, state the equilibrium conditions, and provide the variational inequality formulation. We also present an extension that includes capacity-like constraints. In Section 4, we provide qualitative properties of the model, along with an algorithm. In Section 5, we apply the algorithm to compute solutions to numerical examples in order to illustrate the modeling and algorithmic framework and the types of insights that can be gained. Section 6 summarizes the results and present our conclusions, along with suggestions for future research.

3. The Multiclass, Multiproduct Convalescent Plasma Donor Equilibrium Model

The model consists of m locations at which recovered Covid-19 individuals are located with a typical such origin location denoted by i. There are also n locations at which the convalescent plasma is collected that the donors need to go to, with a typical such destination location denoted by j. As mentioned in the Introduction, there are different types of products that can be produced from the donated convalescent plasma, including that for transfusion into Covid-19 patients. We denote a convalescent plasma product by l and there are r such products. Also, there are o different classes of convalescent plasma donors, with a typical class denoted by k. The network structure for the model is shown in Figure 1.

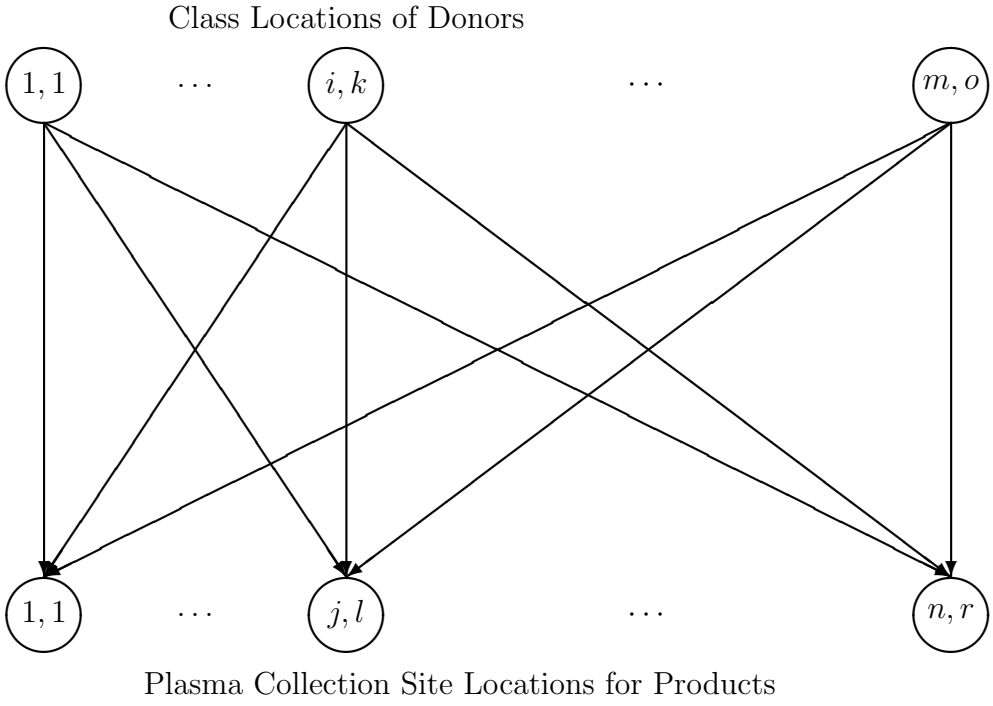

Figure 1: The Network Structure of the Multiclass, Multiproduct Convalescent Plasma Donor Model

All vectors are column vectors. The notation for the model is given in Table 1. Note that we assume that there is a utility function associated with each donor class located at a location and associated with a convalescent plasma product and donation location. In addition, since convenience, safety, risk, time, familiarity, and comfort with a collection site, and possible monetary expenditure are important, we associate a generalized cost for each class at each location in donating for a specific convalescent plasma product at a particular donor site.

Table 1: Notation for the Multiclass, Multiproduct Convalescent Serum Donor Model

Notation	Definition
Q_{ij}^{kl}	the donation flow of convalescent serum for purpose l of class k donor from location i to collection site j. The $\{Q_{ij}^{kl}\}$ elements for all i, j, k, and l are grouped into the vector $Q \in R_+^{mnor}$.
Q_i^k	the nonnegative amount of convalescent serum from potential donors of class k at location i; $k = 1, \ldots, o$; $i = 1, \ldots, m$.
$U_{ij}^{kl}(Q)$	the utility perceived by class k at location i to donate convalescent plasma at location j for product/purpose l; $i = 1, \ldots, m$; $j = 1, \ldots, n$; $k = 1, \ldots, o$; $l = 1, \ldots, r$. We group all the utilities into the vector $U(Q) \in R^{mnor}$.
$c_{ij}^{kl}(Q)$	the generalized cost of class k at location i to go to location j to donate product l of their convalescent plasma, which includes financial cost, time, and risk of class k for $i = 1, \ldots, m$; $j = 1, \ldots, n$; $k = 1, \ldots, o$; $l = 1, \ldots, r$. We group all the generalized costs into the vector $c(Q) \in R^{mnor}$.
λ_i^k	the nonnegative Lagrange multiplier, in effect, associated with the available amount of convalescent plasma potentially to donate by class k located at location i; $i = 1, \ldots, m$; $k = 1, \ldots, o$. We group all the Lagrange multipliers into the vector $\lambda \in R_+^{om}$.

The convalescent serum donations must be nonnegative, that is,

$$Q_{ij}^{kl} \geq 0, \quad \forall i, j, k, l. \tag{1}$$

It is to be noted that the amount of plasma that can be collected from each donor depends on their height, weight, and gender (New York Blood Center (2020)). However, in general, around 3 units of plasma can be obtained from each donor. The flows here denote the number of units of convalescent plasma donated by each class of donors from each location to an organization for a particular purpose.

The convalescent plasma donors seek to identify the product towards which their convalescent plasma will be used as well as the location for their donations. There is a fixed amount of convalescent plasma $\bar{Q}_i^k$ in the recovered population at a location i and class k. The equilibrium conditions which reflect the choices made by the convalescent plasma donors guarantee that if the cost exceed the utility, then the associated flow of convalescent plasma donations will be zero. Also, since the convalescent plasma donor population may not be sufficiently high to clear the market, there is a Lagrange multiplier associated with a class and origin location that will be positive, in equilibrium, if the market clears, and zero, otherwise.

We assume that the utility functions and the generalized cost functions are continuous

with the former being monotonically decreasing and the latter - monotonically increasing.

We define the feasible set $K \equiv \{(Q, \lambda) | \text{ such that } Q \in R_+^{mnor} \text{ and } \lambda \in R_+^{om}\}$. Note that the feasible set K is closed and convex.

The full statement of the governing equilibrium conditions is below.

Definition 1: The Multiclass, Multiproduct Convalescent Plasma Donor Equilibrium Conditions

A vector of multiclass, multiproduct convalescent plasma donations (flows) and a vector of Lagrange multipliers $(Q^*, \lambda^*) \in K$ *are in equilibrium if they satisfy the equilibrium conditions: for each class* k*;* $k = 1, \ldots, o$ *and each product* l*;* $l = 1, \ldots, r$*:*

$$c_{ij}^{kl}(Q^*) \begin{cases} = U_{ij}^{kl}(Q^*) - \lambda_i^{k*}, & \text{if} \quad Q_{ij}^{kl*} > 0, \\ \geq U_{ij}^{kl}(Q^*) - \lambda_i^{k*}, & \text{if} \quad Q_{ij}^{kl*} = 0, \end{cases} \tag{2}$$

and

$$\bar{Q}_i^k \begin{cases} = \sum_{j=1}^n \sum_{l=1}^r Q_{ij}^{kl*}, & \text{if} \quad \lambda_i^{k*} > 0, \\ \geq \sum_{j=1}^n \sum_{l=1}^r Q_{ij}^{kl*}, & \text{if} \quad \lambda_i^{k*} = 0. \end{cases} \tag{3}$$

We now provide a deeper interpretation of equilibrium conditions (2). Specifically, we not thet they can be rewritten as follows. for each class k; $k = 1, \ldots, o$ and each product l; $l = 1, \ldots, r$:

$$\lambda_i^{k*} \begin{cases} = U_{ij}^{kl}(Q^*) - c_{ij}^{kl}(Q^*), & \text{if} \quad Q_{ij}^{kl*} > 0, \\ \geq U_{ij}^{kl}(Q^*) - c_{ij}^{kl}(Q^*), & \text{if} \quad Q_{ij}^{kl*} = 0. \end{cases} \tag{4}$$

From (4) we can see that, for a given class at an origin location, the utility minus the generalized cost is equalized for all plasma product / destination choices that are selected, that is, for those for which there is a positive volume of convalescent plasma donated. And that difference between the utility and the generalized cost exceeds the analogous values for the not selected options, that is, those with zero convalescent plasma donations (flows).

We now provide the variational inequality (VI) formulation of the equilibrium conditions (2) and (3) in the following theorem.

Theorem 1: Variational Inequality Formulation

The vectors of convalescent plasma donations (flows) and Lagrange multipliers satisfy the equilibrium conditions (2) and (3) if and only if they satisfy the variational inequality prob-

lem: determine $(Q^*, \lambda^*) \in K$ *such that*

$$\sum_{i=1}^{m}\sum_{j=1}^{n}\sum_{k=1}^{o}\sum_{l=1}^{r}\left[c_{ij}^{kl}(Q^*) - U_{ij}^{kl}(Q^*) + \lambda_i^{k*}\right] \times \left[Q_{ij}^{kl} - Q_{ij}^{kl*}\right]$$

$$+\sum_{i=1}^{m}\sum_{k=1}^{o}\left[\bar{Q}_i^k - \sum_{j=1}^{n}\sum_{l=1}^{r}Q_{ij}^{kl*}\right] \times \left[\lambda_i^k - \lambda_i^{k*}\right] \geq 0, \quad \forall (Q, \lambda) \in K. \tag{5}$$

Proof: We first establish necessity, that is, we show that if $(Q^*, \lambda^*) \in K$ satisfies equilibrium conditions (2) and (3), then it also satisfies VI (5).

If $(Q^*, \lambda^*) \in K$ satisfies (2), then, for a fixed i, j, k, l, we know that

$$\left[c_{ij}^{kl}(Q^*) - U_{ij}^{kl}(Q^*) + \lambda_i^{k*}\right] \times \left[Q_{ij}^{kl} - Q_{ij}^{kl*}\right] \geq 0, \quad \forall Q_{ij}^{kl} \geq 0. \tag{6}$$

Indeed, if $Q_{ij}^{kl*} > 0$, then the above holds true and the same for $Q_{ij}^{kl*} = 0$.

Summing (6) over all i, j, k, l, we have that

$$\sum_{i=1}^{m}\sum_{j=1}^{n}\sum_{k=1}^{o}\sum_{l=1}^{r}\left[c_{ij}^{kl}(Q^*) - U_{ij}^{kl}(Q^*) + \lambda_i^{k*}\right] \times \left[Q_{ij}^{kl} - Q_{ik}^{kl*}\right] \geq 0, \quad \forall Q \in R_+^{mnor}. \tag{7}$$

Similarly, we know. from equilibrium conditions (3), that, for a fixed i and k:

$$\left[\bar{Q}_i^k - \sum_{j=1}^{n}\sum_{l=1}^{r}Q_{ij}^{kl*}\right] \times \left[\lambda_i^k - \lambda_i^{k*}\right] \geq 0, \quad \forall \lambda_i^k \geq 0. \tag{8}$$

Since (8) holds for any i, k, summation of (8) over all i, k yields:

$$\sum_{i=1}^{m}\sum_{k=1}^{o}\left[\bar{Q}_i^k - \sum_{j=1}^{n}\sum_{l=1}^{r}Q_{ij}^{kl*}\right] \times \left[\lambda_i^k - \lambda_i^{k*}\right] \geq 0, \quad \forall \lambda \in R_+^{mo}. \tag{9}$$

Finally, summation of inequalities (7) and (9) yields VI (5).

We now establish sufficiency, that is, a solution $(Q^*, \lambda^*) \in K$ to VI (5), also satisfies equilibrium conditions (2) and (3).

In (5), we make the following substitutions: we set $\lambda_q^s = \lambda_q^{s*}$ for all $q \neq i$ and $s \neq k$ and $Q_{ij}^{kl} = Q_{ij}^{kl*}$, for all i, j, k, l. This results in:

$$\left[\bar{Q}_i^k - \sum_{j=1}^{n}\sum_{l=1}^{r}Q_{ij}^{kl*}\right] \times \left[\lambda_i^k - \lambda_i^{k*}\right] \geq 0, \quad \forall \lambda_i^k \geq 0, \tag{10}$$

which implies that equilibrium condition (3) holds.

Now, we set $\lambda_i^k = \lambda_i^{k*}$ for all i, k, in VI (5) and we set $Q_{qt}^{sh} = Q_{qt}^{sh*}$ for all $q, t, s, h \neq i, j, k, l$ and substitute into VI (5), which yields:

$$\left[c_{ij}^{kl}(Q^*) - U_{ij}^{kl}(Q^*) + \lambda_i^{k*}\right] \times \left[Q_{ij}^{kl} - Q_{ij}^{kl*}\right] \geq 0, \quad \forall Q_{ij}^{kl} \geq 0, \tag{11}$$

and inequality (11) clearly implies that equilibrium condition (2) holds. The proof is complete. □

3.1 An Extension to Include Capacities

It is important to recognize that some collection sites may be capacitated. Hence, we introduce some new notation. We let cap_j denote the maximum amount of plasma donations that can be handled at collection site j and we let $\mathcal{S}$ be the set of such sites j. We assume that there are $n_{\mathcal{S}}$ elements in the set $\mathcal{S}$. Also, we introduce the Lagrange multiplier γ_j for each collection site $j \in \mathcal{S}$ and we group the Lagrange multipliers γ_j into the vector $\gamma \in R_+^{n_{\mathcal{S}}}$. We define the feasible set $K^2 \equiv \{(Q, \lambda, \gamma) | \text{ such that } Q \in R_+^{mnor}, \lambda \in R_+^{om}, \gamma \in R_+^{n_{\mathcal{S}}}\}$.

In the capacitated extension of the above model, the equilibrium conditions are now as below.

Definition 2: The Capacitated Multiclass, Multiproduct Convalescent Plasma Donor Equilibrium Conditions

A vector of multiclass, multiproduct convalescent plasma donations (flows) and vectors of Lagrange multipliers $(Q^*, \lambda^*, \gamma^*) \in K^2$ are in equilibrium if they satisfy the equilibrium conditions: for each class k; $k = 1, \ldots, o$, each product l; $l = 1, \ldots, r$, for donors at i; $i = 1, \ldots, m$, and for $j \in \mathcal{S}$:

$$c_{ij}^{kl}(Q^*) \begin{cases} = U_{ij}^{kl}(Q^*) - \lambda_i^{k*} - \gamma_j^*, & \text{if} \quad Q_{ij}^{kl*} > 0, \\ \geq U_{ij}^{kl}(Q^*) - \lambda_i^{k*} - \gamma_j^*, & \text{if} \quad Q_{ij}^{kl*} = 0, \end{cases} \tag{12a}$$

whereas for each class k; $k = 1, \ldots, o$, each product l; $l = 1, \ldots, r$, for donors at i; $i = 1, \ldots, m$, and for $j \notin \mathcal{S}$:

$$c_{ij}^{kl}(Q^*) \begin{cases} = U_{ij}^{kl}(Q^*) - \lambda_i^{k*}, & \text{if} \quad Q_{ij}^{kl*} > 0, \\ \geq U_{ij}^{kl}(Q^*) - \lambda_i^{k*}, & \text{if} \quad Q_{ij}^{kl*} = 0, \end{cases} \tag{12b}$$

and for $j \in \mathcal{S}$:

$$cap_j \begin{cases} = \sum_{i=1}^{m} \sum_{k=1}^{o} \sum_{l=1}^{r} Q_{ij}^{kl*}, & \text{if} \quad \gamma_j^* > 0, \\ \geq \sum_{i=1}^{m} \sum_{k=1}^{o} \sum_{l=1}^{r} Q_{ij}^{kl*}, & \text{if} \quad \gamma_j^* = 0, \end{cases} \tag{13}$$

with (3), as before, holding for all j, that is,

$$\bar{Q}_i^k \begin{cases} = \sum_{j=1}^n \sum_{l=1}^r Q_{ij}^{kl*}, & \text{if} \quad \lambda_i^{k*} > 0, \\ \geq \sum_{j=1}^n \sum_{l=1}^r Q_{ij}^{kl*}, & \text{if} \quad \lambda_i^{k*} = 0. \end{cases} \tag{14}$$

The following variational inequality formulation of the above equilibrium conditions is immediate.

Theorem 2: Variational Inequality Formulation of the Capacitated Model

A vector of multiclass, multiproduct convalescent plasma donations (flows) and a vector of Lagrange multipliers $(Q^*, \lambda^*, \gamma^*) \in K^2$ satisfy the equilibrium conditions (12a), 12(b), (13), and (14) if and only if they satisfy the variational inequality problem: determine $(Q^*, \lambda^*, \gamma^*) \in K^2$ such that

$$\sum_{i=1}^m \sum_{j \in S} \sum_{k=1}^o \sum_{l=1}^r \left[c_{ij}^{kl}(Q^*) - U_{ij}^{kl}(Q^*) + \lambda_i^{k*} + \gamma_j^* \right] \times \left[Q_{ij}^{kl} - Q_{ij}^{kl*} \right]$$

$$+ \sum_{i=1}^m \sum_{j \notin S} \sum_{k=1}^o \sum_{l=1}^r \left[c_{ij}^{kl}(Q^*) - U_{ij}^{kl}(Q^*) + \lambda_i^{k*} \right] \times \left[Q_{ij}^{kl} - Q_{ij}^{kl*} \right]$$

$$+ \sum_{j \in S} \left[cap_j - \sum_{i=1}^m \sum_{k=1}^o \sum_{l=1}^r Q_{ij}^{kl*} \right] \times \left[\gamma_j - \gamma_j^* \right] + \sum_{i=1}^m \sum_{k=1}^o \left[\bar{Q}_i^k - \sum_{j=1}^n \sum_{l=1}^r Q_{ij}^{kl*} \right] \times \left[\lambda_i^k - \lambda_i^{k*} \right] \geq 0,$$

$$\forall (Q^*, \lambda^*, \gamma^*) \in K^2. \tag{15}$$

We now put variational inequality (5) into standard form (cf. Nagurney (1999)): determine $X^* \in \mathcal{K}$ such that

$$\langle F(X^*), X - X^* \rangle \geq 0, \quad \forall X \in \mathcal{K}, \tag{16}$$

where F is a given continuous function from $\mathcal{K}$ to R^N, $\mathcal{K}$ is a given closed convex set, and $\langle \cdot, \cdot \rangle$ denotes the inner product in N-dimensional Euclidean space.

We set $\mathcal{K} \equiv K$, $X \equiv (Q, \lambda)$, and $N = mnor + mo$. Also, we define the vector $F \equiv (F_1, F_2)$, where the components of F_1 consist of the elements: $c_{ij}^{kl}(Q) - U_{ij}^{kl}(Q) + \lambda_i^k$, $\forall i, j, k, l$, and the components of F_2 consist of the elements: $\bar{Q}_i^k - \sum_{j=1}^n \sum_{l=1}^r Q_{ij}^{kl}$, $\forall i, k$. Then, clearly, VI(5) coincides with VI(16), with the above definitions.

VI (15) can, analogously, also be put into standard form (15), but with the expansion of the definitions of the vectors X and $F(X)$ and also of R^N since in the constrained case we have additional Lagrange multipliers in the vector γ.

4. Qualitative Properties and the Algorithm

We now discuss some properties of the model, specifically, those that guarantee that the conditions for convergence of the modified projection method (cf. Korpelevich (1977) and Nagurney (1999)) that we use to compute solutions to numerical examples in this next section are met. Specifically, the algorithm is guaranteed to converge to a solution of variational inequality (16) if the function $F(X)$ that enters the VI is monotone and Lipschitz continuous, and that a solution exists. It was recently applied to compute solutions to a stochastic game theory model for disaster relief by Nagurney, Salarpour, and Nagurney (2020).

Recall that the function $F(X)$ is said to be monotone, if

$$\langle F(X^1) - F(X^2), X^1 - X^2 \rangle \geq 0, \quad \forall X^1, X^2 \in \mathcal{K}. \tag{17}$$

The function $F(X)$ is Lipschitz continuous, if there exists a constant $L > 0$, known as the Lipschitz constant, such that

$$\|F(X^1) - F(X^2)\| \leq L\|X^1 - X^2\|, \quad \forall X^1, X^2 \in \mathcal{K}. \tag{18}$$

We now write $\langle F(X^1) - F(X^2), X^1 - X^2 \rangle$ for $F(X)$ as defined for VI (5) and obtain, after algebraic simplification:

$$\sum_{i=1}^{m}\sum_{j=1}^{n}\sum_{k=1}^{o}\sum_{l=1}^{r}((c_{ij}^{kl}(Q^1) - U_{ij}^{kl}(Q^2)) - (c_{ij}^{kl}(Q^2) - U_{ij}^{kl}(Q^2)) \times (Q_{ij}^{kl1} - Q_{ij}^{kl2}). \tag{19}$$

And, under our previously imposed assumptions that $c(Q)$ is monotone increasing and that $U(Q)$ is monotone decreasing it follows that the term in (19) is greater than or equal to zero and, hence, $F(X)$ is monotone. Under the same assumptions, the $F(X)$ for VI (15) is also monotone.

As for Lipschitz continuity, if both the generalized cost and the utility functions have bounded second order partial derivatives, then $F(X)$ will be Lipschitz continuous (see also Nagurney and Zhang (1996) and Nagurney (1999)).

The iterative steps of the modified projection method, with τ denoting an iteration counter, are as follows:

The Modified Projection Method

Step 0: Initialization

Initialize with $X^0 \in \mathcal{K}$. Set the iteration counter $\tau := 1$ and let β be a scalar such that $0 < \beta \leq \frac{1}{L}$, where L is the Lipschitz constant.

Step 1: Computation

Compute $\bar{X}^\tau$ by solving the variational inequality subproblem:

$$\langle \bar{X}^\tau + \beta F(X^{\tau-1}) - X^{\tau-1}, X - \bar{X}^\tau \rangle \geq 0, \quad \forall X \in \mathcal{K}. \tag{20}$$

Step 2: Adaptation

Compute X^τ by solving the variational inequality subproblem:

$$\langle X^\tau + \beta F(\bar{X}^\tau) - X^{\tau-1}, X - X^\tau \rangle \geq 0, \quad \forall X \in \mathcal{K}. \tag{21}$$

Step 3: Convergence Verification

If $|X^\tau - X^{\tau-1}| \leq \epsilon$, with $\epsilon > 0$, a pre-specified tolerance, then stop; otherwise, set $\tau := \tau + 1$ and go to Step 1.

The modified projection method for both the model governed by VI (5) and that capacitated extension one governed by VI (15) yields closed form expressions for the convalescent plasma product donations and for the Lagrange multipliers in both Steps (20) and (21). hence, these are nice features for implementation.

5. Numerical Examples

In this Section, we apply the modified projection method to compute solutions to numerical examples. The algorithm was implemented in FORTRAN and the computer system used was a Linux system at the University of Massachusetts Amherst. We initialized the algorithm by setting all the donation flows and the Lagrange multipliers to 0.00. The convergence condition for all the examples was that the absolute value of two successive variable iterates was less than or equal to 10^{-7}.

The model developed in this paper can be applied to any region or country that is recruiting convalescent plasma donors. The examples here, although stylized, are inspired

by the Covid-19 outbreak in New York City, the areas that have been affected, the number of recovered patients, and also the availability of collection sites for convalescent plasma products. We assume the time frame for the model to be a month. Hence, the flows obtained here denote the number of units of convalescent plasma donated in a month. The American Red Cross which began collection with FDA's approval in early April reportedly had collected around 200 units of convalescent plasma towards the end of the month (Pawlowski (2020)). The values we obtain from the numerical examples are close to the above figure.

The series of numerical examples are constructed in increasing order of complexity.

Example 1: Single Class, Two Origin Locations, and a Single Nonprofit Collection Location

The first example consists of a single class of donor at two locations: Williamsburg, Brooklyn, corresponding to origin location 1 and Corona, Queens, corresponding to origin location 2. These location areas are among the most severely affected neighborhoods in New York (Aleccia (2020), Chadha (2020)). There is a single collection site for convalescent plasma as depicted in Figure 2 which we associate with a nonprofit organization such as Mount Sinai Hospital which spearheaded the convalescent plasma treatment in New York City (Ferguson et al. (2020)).

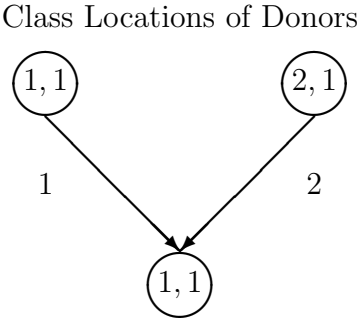

Figure 2: Network Topology for Example 1

For completeness, and easy reference, we also map the donation flow variable with the numbered link in Figure 2. Specifically, Q_{11}^{11} is the flow on link 1 and Q_{21}^{11} is the flow on link 2. Recall that we use Q_{ij}^{kl} notation for the convalescent plasma donations of those located at origin location i of class k donating at collection site j for use in product l.

The available supplies (bounds) at the origin locations of the convalescent plasma that can be donated are:

$$\bar{Q}_1^1 = 100.00, \quad \bar{Q}_2^1 = 150.00.$$

The generalized cost functions are:

$$c_{11}^{11}(Q) = 2Q_{11}^{11} + 2, \quad c_{21}^{11}(Q) = 3Q_{21}^{11} + 3.$$

The utility functions are:

$$U_{11}^{11}(Q) = -1Q_{11}^{11} + 1000, \quad U_{21}^{11}(Q) = -1Q_{21}^{11} + 1500.$$

The modified projection method converged to the following equilibrium solution:

$$Q_{11}^{11*} = 100.00, \quad Q_{21}^{11*} = 150.00,$$

with

$$\lambda_1^{1*} = 698.00, \quad \lambda_2^{1*} = 897.00.$$

The utilities at the equilibrium solution are:

$$U_{11}^{11}(Q^*) = 900.00, \quad U_{21}^{11}(Q^*) = 1350.00.$$

In this example, we can see that the donors at both origin locations choose to donate all their available convalescent plasma. The Lagrange multipliers are, hence, positive. We are seeing this in practice, that those who have recovered from Covid-19 are seeking to give back and help others through donations of convalescent plasma.

Example 2: Single Class, Two Origin Locations, and Two Nonprofit Collection Locations

Example 2 is constructed from Example 1 and has the same data but with the addition of new data to handle a new collection site for convalescent plasma for another nonprofit. This new collection site, at destination location 2, is perceived as the New York Blood Center site in Long Island City which is closer to the donor origin locations. The network topology for this example is depicted in Figure 3.

Note that new links 3 and 4 have been added joining the origin locations with the new collection site in Figure 3. The plasma donation variable associated with link 3 is: Q_{12}^{11}, whereas that for link 4 is: Q_{22}^{11}.

The generalized cost functions associated with the added collection site (and the new links) are:

$$c_{12}^{11}(Q) = 2Q_{12}^{11} + 1, \quad c_{22}^{11}(Q) = 4Q_{22}^{11} + 2.$$

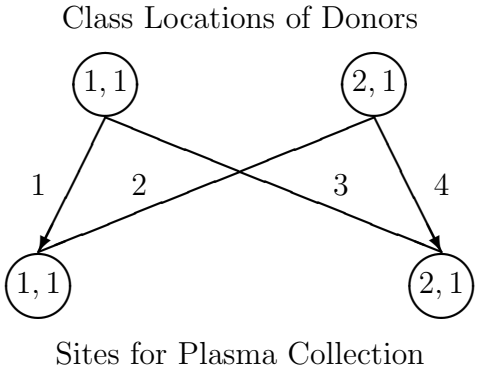

Figure 3: Network Topology for Example 2

The utility functions, in turn, are:

$$U_{12}^{11}(Q) = -2Q_{12}^{11} + 2000, \quad U_{22}^{11}(Q) = -1Q_{22}^{11} + 2000.$$

The utility functions have higher fixed terms at the new collection site than at the first one since the class of donors feels that the specialization in blood services is a positive feature of the site. Since there could be traffic, even in the pandemic, this is captured by a higher coefficient of "4" preceding the donation flow Q_{22}^{11}.

The modified projection method converged to the following equilibrium solution:

$$Q_{11}^{11*} = 0.00, \quad Q_{21}^{11*} = 27.67, \quad Q_{12}^{11*} = 100.00, \quad Q_{22}^{11*} = 122.33,$$

and

$$\lambda_1^{1*} = 1599.00, \quad \lambda_2^{1*} = 1386.33.$$

The utilities at the equilibrium solution are:

$$U_{11}^{11}(Q^*) = 1000.00, \quad U_{21}^{11}(Q^*) = 1472.33, \quad U_{12}^{11}(Q^*) = 1800.00, \quad U_{22}^{11}(Q^*) = 1877.67.$$

Observe that with the new collection site, the donors at the first origin location now donate all their convalescent plasma to the new collection site. Also, the donors at the second origin site donate the majority of their plasma to the new site. Again, all the available plasma is donated and the Lagrange multipliers are positive.

Example 3 - Single Class, Two Origin Locations, and Three Collection Locations, with One Being a For Profit One Collecting for Another Product

Example 3 has the same data as Example 2 but now we consider the following scenario. A for profit organization such as Grifols or Takeda has heard of the number of convalescent

plasma donations at the second collection point and has decided to locate very near there. The convalescent plasma will not be for use soon thereafter in patients but, rather, for a new product. The new collection site 3 and the associated links (links 5 and 6) destined to it are depicted in the network topology representing this example in Figure 4. The plasma donation variable associated with link 5 is: Q_{13}^{12} and that with link 6: Q_{23}^{12}.

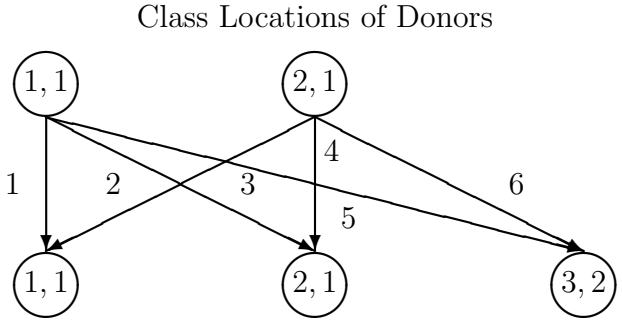

Figure 4: Network Topology for Example 3

The data for Example 3 was the same as that for Example 2 with the following additions for the new collection site which collects for a different product geared to making a profit.

The added generalized cost functions associated with the new collection site associated with a for profit organization are:

$$c_{13}^{12}(Q) = 2Q_{13}^{12} + 1, \quad c_{23}^{12}(Q) = 4Q_{23}^{12} + 2.$$

The added utility functions, in turn, are:

$$U_{13}^{12}(Q) = -1Q_{13}^{12} + 2500, \quad U_{23}^{12}(Q) = -1Q_{23}^{12} + 2500.$$

Note that the utility function fixed terms associated with donating to the new collection site are higher than those fixed terms associated with the other nonprofit collection sites since donors now get financial compensation for their convalescent plasma donations at the third destination site. Also, note that the analogous generalized cost functions are the same since the location of the collection site is essentially at the same place as the second collection site.

The modified projection method converged to the following equilibrium solution:

$$Q_{11}^{11*} = 0.00, \quad Q_{21}^{11*} = 0.00, \quad Q_{12}^{11*} = 0.00, \quad Q_{22}^{11*} = 25.00,$$

$$Q_{13}^{12*} = 100.00, \quad Q_{23}^{12*} = 125.00,$$

and

$$\lambda_1^{1*} = 2199.00, \quad \lambda_2^{1*} = 1873.00.$$

The utilities at the equilibrium solution are:

$$U_{11}^{11}(Q^*) = 1000.00, \quad U_{21}^{11}(Q^*) = 1500.00, \quad U_{12}^{11}(Q^*) = 2000.00, \quad U_{22}^{11}(Q^*) = 1975.00,$$

$$U_{13}^{12}(Q^*) = 2400.00, \quad U_{23}^{12}(Q^*) = 2375.00.$$

The donors at origin location 1 now donate all their convalescent plasma to the for profit collection site. The donors at the second origin location donate the majority of their convalescent plasma also to the for profit collection site, and a much smaller amount to the second collection site. Clearly, the nonprofits lose in terms of convalescent plasma donations due to the competition from the profit organization.

Example 4 - Variant of Example 3

In Example 4, we consider the following scenario. The donors at the second origin location are now a bit embarrassed by those in their community in that they are donating so much convalescent plasma to the for profit organization.

Hence, their utility function associated with donating to the for profit has now been modified to:

$$U_{23}^{12}(Q) = -1Q_{23}^{12} - .7Q_{22}^{11} + 2500.$$

The modified utility function reflects that the utility function is also decreasing in the number of convalescent plasma donations from that origin location to the second donation site.

The modified projection method now yielded to the following equilibrium solution:

$$Q_{11}^{11*} = 0.00, \quad Q_{21}^{11*} = 0.00, \quad Q_{12}^{11*} = 0.00, \quad Q_{22}^{11*} = 26.88,$$

$$Q_{13}^{12*} = 100.00, \quad Q_{23}^{12*} = 123.12,$$

and

$$\lambda_1^{1*} = 2199.00, \quad \lambda_2^{1*} = 1863.59.$$

Once can now that there is a positive amount of convalescent plasma that is being "switched" from being donated to the for profit organization to the nonprofit one at the second collection site. All the plasma at both origin locations is fully donated with the Lagrange multipliers, again, being both positive.

The utilities at the equilibrium solution are now:

$$U_{11}^{11}(Q^*) = 1000.00, \quad U_{21}^{11}(Q^*) = 1500.00, \quad U_{12}^{11}(Q^*) = 2000.00, \quad U_{22}^{11}(Q^*) = 1973.12,$$

$$U_{13}^{12}(Q^*) = 2400.00, \quad U_{23}^{12}(Q^*) = 2358.06.$$

Example 5 and Variant - Addition of a New Class

Example 5 has the same data as Example 4 but now we introduce a new class 2 that, because of specific criteria that must be satisfied, is not able to donate their convalescent plasma for direct infusion into Covid-19 patients but, rather, can still donate for another product and that product is managed by the for profit organization at its collection site 3. The network topology is as in Figure 5. The new link is link 7 and it is associated with the plasma donation variable: Q_{23}^{22}.

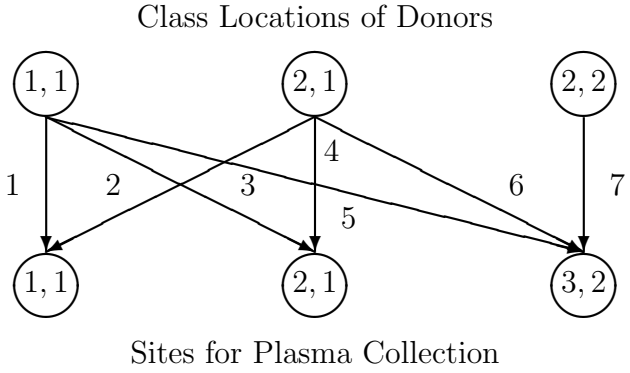

Figure 5: Network Topology for Example 5

The additional data associated with link 7 are as follows.

The generalized link cost is:

$$c_{23}^{22}(Q) = 6Q_{23}^{22} + 5$$

and the utility function is:

$$U_{23}^{22}(Q) = -1Q_{23}^{22} + .4Q_{23}^{12} + 2000.$$

Also, we have:

$$\bar{Q}_2^2 = 140.00.$$

The above generalized link cost captures culture barriers in that this class may be reluctant to travel, whereas the utility function captures that there is a positive effect, due to

familiarity, associated with the other class from the same origin location donating to the for profit collection site.

The modified projection method yielded the equilibrium solution:

$$Q_{11}^{11*} = 0.00, \quad Q_{21}^{11*} = 0.00, \quad Q_{12}^{11*} = 0.00, \quad Q_{22}^{11*} = 26.88,$$

$$Q_{13}^{12*} = 100.00, \quad Q_{23}^{12*} = 123.12, \quad Q_{23}^{22*} = 140.00,$$

and

$$\lambda_1^{1*} = 2199.00, \quad \lambda_2^{1*} = 1864.00, \quad \lambda_2^{2*} = 1064.24.$$

The new class of donor donates its entire supply of convalescent plasma and the equilibrium Lagrange multiplier is positive.

The utilities at the equilibrium solution are now:

$$U_{11}^{11}(Q^*) = 1000.00, \quad U_{21}^{11}(Q^*) = 1500.00, \quad U_{12}^{11}(Q^*) = 2000.00, \quad U_{22}^{11}(Q^*) = 1973.12,$$

$$U_{12}^{13}(Q^*) = 2400.00, \quad U_{23}^{12}(Q^*) = 2358.06, \quad U_{23}^{22}(Q^*) = 1909.25.$$

We then modified the new class donors' utility function to signify a decrease in utility associated with donating as follows:

$$U_{23}^{22}(Q) = -1Q_{23}^{22} + .4Q_{23}^{12} + 500.$$

The modified projection method converged to an equilibrium solution, which differed from the one immediately above in that:

$$Q_{23}^{22*} = 77.75, \quad \lambda_2^{2*} = 0.00$$

with $U_{23}^{22}(Q^*) = 471.50$.

Observe that now class 2 does not donate all of the convalescent plasma that it can and, hence, the associated Lagrange multiplier is equal to 0.00.

Example 6 - Bound On Location 3 Collection Site

Example 6 was inspired by the following scenario. The workers at collection site 3 have been falling ill with Covid-19 and there are, hence, fewer labor resources available for handling the convalescent plasma donations at this for profit organization collection site.

The solutions to all the preceding examples satisfied the unconstrained version VI (5), whereas the governing equilibrium conditions for this constrained example satisfy VI (15),

where recall that we have an additional Lagrange multiplier γ associated with the bound on the flows to the destination location under the capacity constraint.

There is, hence, a capacity at this site of: $cap_3 = 300.00$, which is imposed on donations/flows to node $(3, 2)$ in Figure 5. Hence, links 5, 6, and 7 may be affected with associated variables of: Q_{13}^{12}, Q_{23}^{12}, and Q_{23}^{22}.

The remainder of the data is as in Example 5.

The computed equilibrium solution for this example is:

$$Q_{11}^{11*} = 0.00, \quad Q_{21}^{11*} = 0.00, \quad Q_{12}^{11*} = 23.74, \quad Q_{22}^{11*} = 66.26,$$

$$Q_{13}^{12*} = 76.26, \quad Q_{23}^{12*} = 83.74, \quad Q_{23}^{22*} = 140.00,$$

$$\lambda_1^{1*} = 1904.02, \quad \lambda_2^{1*} = 1666.70, \quad \lambda_2^{2*} = 682.28,$$

and $\gamma_3^* = 366.21$.

Observe that all the Lagrange multipliers are positive and, therefore, on the supply side all of the convalescent plasma available is donated and on the demand side, the for profit collection site is at its capacity for handling the plasma donated there.

We see that, as compared to the results in Example 5, that now there is a positive amount of convalescent plasma donated by class 1 and origin location 2 to nonprofit collection site 1 and an increase in convalescent plasma donations from this class and location to collection site 2. However, because of the capacity on collection site 3, the volume of plasma donations there decreases from donors of class 1. Class 2, which is unable to donate for immediate transfusion purposes, again, donates all of its plasma to the for profit site 3.

Some of the insights gained from the above numerical examples, although stylized are:

1. It is important to make the experience of donating convalescent plasma as positive as feasible since a decrease in a utility function fixed term can impact donations.

2. Care should be taken when a for profit moves in since convalescent plasma donors may shift their donations from nonprofit organizations to a for profit one.

3. Proximity matters and convenience of collection sites.

4. Availability of labor needed for the collection process during the pandemic and capacities of the collection sites play an important role. Organizations collecting convalescent plasma need to have the resources to collect from the donors.

6. Summary and Conclusions and Suggestions for Future Research

In this paper, we developed a multiclass, multiproduct equilibrium model to study the behavior of convalescent plasma donors in the Covid-19 pandemic. As more and more countries across the globe approve clinical trials for convalescent plasma therapy to fight the Covid-19 pandemic and as collections of this life-saving product gain momentum, it will be critical to understand how different classes of donors located at different sites choose to donate to different organizations. Antibody-rich plasma from recovered Covid-19 patients is not only being used to treat severely ill patients, but also to develop other products such as hyper-immune globulin. Each location in our model has a fixed population of convalescent plasma donors who meet the eligibility criteria. The donor population can be separated into several classes based on their motivation to donate and the product for which they are donating at a specific location. Preferencess of each class of donor at an origin location for donating for a convalescent plasma product at a collection site is captured in the utility functions. While people make charitable donations driven by altruism, there are tangible factors associated with the effort to donate that might deter donors. It requires time and cost to travel to a plasma collection site to provide donations. Often donors have to wait for their turn and the collection process itself takes about an hour. Moreover, during a pandemic there are risks of infection associated with traveling, specially if the collection sites are far from the donor's location as well as the possibility of an accident. All these important factors affecting donor decisions are captured in our generalized cost functions.

To the best of our knowledge this is the first model to capture competition for convalescent plasma between nonprofit organizations such as blood banks and hospitals, and for profit organizations such as pharmaceutical companies that are working on the development of plasma derived products. An extension of the convalescent plasma model is provided to include capacity restrictions at collection sites. We provide equilibrium conditions for both capacitated and uncapacitated models. Qualitative properties of the model and the algorithmic framework of modified projection method are also outlined. The algorithm is implemented and applied to solve a series of numerical examples that explore several scenarios with varying levels of complexity. The results obtained from these numerical examples reveal how nonprofit organizations might lose donations due to competition from for profit organizations that provide monetary compensations to donors. The insights obtained from this analysis can help policy makers understand the behavior pattern of convalescent plasma donors under different circumstances.

As the studies on convalescent plasma therapy make progress and more data are accessible on the availability and collection of convalescent plasma, our model can be further tested

using real data. Another possible extension of this work would involve capturing the stochastic nature of the supply and demand for convalescent plasma. Furthermore, since there is the possibility of repeat donations of convalescent plasma, adding that feature to the model would be interesting. Constructing a game theory model with objective functions for the nonprofit and the for profit organizations competing for a limited amount of convalescent plasma would also be worthwhile.

Every global tragedy in human history dating back to World War II has paved the way for scientific innovation, technological advancement, and better understanding of the psyche of society at large. This Covid-19 pandemic is not any different. The Operations Research and Management Science community has the skill set and mathematical and computational tools needed to analyze the evolving situation with the outbreak of the disease. Research on the pandemic using Operations Research and Management Science tools is important and can help inform and guide decision makers also in the area of public policy. With this paper we contribute to the literature with the development of a new model for convalescent plasma in a unique market that has arisen in the Covid-19 pandemic. The model handles different classes of donors, as well as different convalescent plasma products, and allows for the investigation, in its computational form, a multiplicity of scenarios such as the impact of the addition of classes, the addition of donor origin locations, and the addition of nonprofit collection sites and a for profit competitor collection site. Of course, sensitivity analysis of the underlying functions is also made possible and we illustrated this as well in the form of changes in utility functions.

Acknowledgments

This paper is dedicated to essential workers, including the excellent systems administrators in Engineering Computer Services at UMass Amherst, who even in a pandemic assisted the first author, notably, Jose Figueroa and Stephen Cumberbatch, and to all the tech workers, healthcare workers, first responders, grocery store workers, and freight service providers, whose dedication and extraordinary efforts during the Covid-19 pandemic helped to sustain us. Thank you.

Statement

No funding was provided for this work.

Conflict of Interest: The authors declare that they have no conflict of interest.

References

Aleccia, J., 2020. Market for blood plasma from COVID-19 survivors heats up. NPR, May 11. Available at: https://www.npr.org/sections/health-shots/2020/05/11/852354920/market-for-blood-plasma-from-covid-19-survivors-heats-up.

American Red Cross, 2020. FAQ: COVID-19 Convalescent Plasma.
Available online: https://www.redcrossblood.org/faq.html#donating-blood-covid-19-convalescent-plasma.

Andreoni, J., 1990. Impure altruism and donations to public goods: A theory of warm-glow giving. The Economic Journal 10(401), 464-477.

Baveja, A., Kapoor, A., Melamed, B., 2020. Stopping Covid-19: A pandemic-management service value chain approach. Annals of Operations Research, in press. Available online: https://doi.org/10.1007/s10479-020-03635-3.

Beasley, D., 2020. Donated plasma benefits COVID-19 patients in small U.S. study. Reuters, May 22. Available online: https://www.reuters.com/article/us-health-coronavirus-plasma/donated-plasma-benefits-covid-19-patients-in-small-u-s-study-idUSKBN22Y303.

Bloch, E.M., Shoham, S., Casadevall, A., Sachais, B.S., Shaz, B., Winters, J.L., van Buskirk, C., Grossman, B.J., Joyner, M., Henderson, J.P., Pekosz, A., 2020. Deployment of convalescent plasma for the prevention and treatment of COVID-19. The Journal of Clinical Investigation, in press.

Bradley, J. 2020. Blood samples, vital for antibody tests, sold at exorbitant rates. May 1, The New York Times. Available at: https://www.nytimes.com/2020/05/01/world/europe/coronavirus-blood-samples.html.

Casadevall, A., Pirofski, L.A., 2020. The convalescent sera option for containing COVID-19. The Journal of Clinical Investigation 130(4), 1545-1548.

Chadha, J., 2020. New York City's most crowded neighborhoods are often hardest hit by coronavirus. Politico, April 11.
Available online: https://www.politico.com/states/new-york/albany/story/2020/04/11/new-york-citys-most-crowded-neighborhoods-are-often-hardest-hit-by-coronavirus-1274875.

Craig, A.C., Garbarino, E., Heger, S.A., Slonim, E., 2017. Waiting to give: Stated and revealed preferences. Management Science 63(11), 3672-3690.

Davies, E., 2020. As states begin to reopen, blood banks brace for surge in demand. The Washington Post, May 22. Available online: https://www.washingtonpost.com/local/as-states-begin-to-reopen-blood-banks-brace-for-surge-in-demand/2020/05/22/0dbd25ec-9add-11ea-89fd-28fb313d1886_story.html.

Duan, K., Liu, B., Li, C., Zhang, H., Yu, T., Qu, J., Zhou, M., Chen, L., Meng, S., Hu, Y., Peng, C., 2020. Effectiveness of convalescent plasma therapy in severe COVID-19 patients. Proceedings of the National Academy of Sciences 117(17), 9490-9496.

Dutta, P., Nagurney, A., 2019. Multitiered blood supply chain network competition: Linking blood service organizations, hospitals, and payers. Operations Research for Health Care 23, 100230.

European Blood Alliance, 2020. Convalescent plasma (CCP).
Available online: https://europeanbloodalliance.eu/activities/convalescent-plasma-cpp/.

Evans, R., Ferguson, E., 2013. Defining and measuring blood donor altruism: A theoretical approach from biology, economics and psychology. Vox Sanguinis 106(2), 118-26.

Fazli-Khalaf, M., Khalilpourazari, S., Mohammadi, M., 2019. Mixed robust possibilistic flexible chance constraint optimization model for emergency blood supply chain network design. Annals of Operations Research 283, 1079-1109.

Ferguson, C., McFadden, C., Martinez, D., 2020. Plasma treatment being tested in New York may be coronavirus 'game changer'. NBC News, April 6.
Available online: https://www.nbcnews.com/health/health-news/plasma-treatment-being-tested-new-york-may-be-coronavirus-gamechanger-n1178436.

Ferguson, C., McFadden, C., Martinez, D., Schapiro, R., 2020. Convalescent plasma is safe to treat COVID-19: nationwide study. NBC News, May 14.
Available online: https://www.nbcnews.com/health/health-news/convalescent-plasma-safe-treat-covid-19-nationwide-study-n1206126.

Food and Drug Administration, 2020a. COVID-19 convalescent plasma collection: Donor eligibility, processing, labeling, and distribution. April 4. Available at: https://www.fda.gov/vaccines-blood-biologics/investigational-new-drug-ind-or-device-exemption-ide-process-cber/recommendations-investigational-covid-19-convalescent-plasma.

Food and Drug Administration, 2020b. Recommendations for investigational COVID-19 convalescent plasma. May 1.

Available online: https://www.fda.gov/emergency-preparedness-and-response/coronavirus-disease-2019-covid-19/donate-covid-19-plasma.

Gillespie, T.W., Hillyer, C. D., 2002. Blood donors and factors impacting the blood donation decision. Transfusion Medicine Reviews 16(2), 115-130.

Hererra, T. 2020. What is convalescent blood plasma, and why do we care about it? April 24, The New York Times. Available at: https://www.nytimes.com/2020/04/24/smarter-living/coronavirus-convalescent-plasma-antibodies.html.

Hosseini-Motlagh, S.M., Samani, M.R.G., Cheraghi, S., 2020. Robust and stable flexible blood supply chain network design under motivational initiatives. Socio-Economic Planning Sciences 70, 100725.

Ivanov, D., 2020. Viable supply chain model: integrating agility, resilience and sustainability perspectives—lessons from and thinking beyond the COVID-19 pandemic. Annals of Operations Research. Available online: https://doi.org/10.1007/s10479-020-03640-6.

Kaplan, E.H., 2020 Containing 2019-nCoV (Wuhan) coronavirus. Health Care Management Science, 1-4. Available online: https://doi.org/10.1007/s10729-020-09504-6.

Kessler, J.B., Roth, A.E., 2012. Organ allocation policy and the decision to donate. American Economic Review 102(5), 2018-2047.

Khalilpourazari, S., Khamseh, A.A., 2019. Bi-objective emergency blood supply chain network design in earthquake considering earthquake magnitude: a comprehensive study with real world application. Annals of Operations Research 283, 355-393.

Korcok, M., 2002. Blood donations dwindle in US after post-Sept. 11 wastage publicized. CMAJ: Canadian Medical Association Journal 167(8), 907.

Korpelevich, G.M., 1977. The extragradient method for finding saddle points and other problems. Matekon 13, 35-49.

Lacetera, N., Macis, M., Slonim, R., 2013. Economic rewards to motivate blood donations. Science 340(6135), 927-928.

Life Serve Blood Center, 2020. Questions about convalescent plasma. Available online: https://www.lifeservebloodcenter.org/donate/recovered-covid-19-patient-plasma-donation/questions-convalescent-plasma/.

Mair-Jenkins, J., Saavedra-Campos, M., Baillie, J.K., Cleary, P., Khaw, F.M., Lim, W.S., Makki, S., Rooney, K.D., Convalescent Plasma Study Group, Nguyen-Van-Tam, J.S. and Beck, C.R., 2015. The effectiveness of convalescent plasma and hyperimmune immunoglobulin for the treatment of severe acute respiratory infections of viral etiology: a systematic review and exploratory meta-analysis. The Journal of Infectious Diseases 211(1), 80-90.

Masoumi, A.H., Yu, M., Nagurney, A., 2017. Mergers and acquisitions in blood banking systems: A supply chain network approach. International Journal of Production Economics 193, 406-421.

MD Bureau, 2020. ICMR Gets National Ethics Committee Nod For COVID-19 Plasma Therapy. Medical Dialogues, May 9. Available online: https://medicaldialogues.in/news/health/government-policies/icmr-gets-national-ethics-committee-nod-for-covid-19-plasma-therapy-65599.

Muggy, L., Stamm, J.L.H., 2014. Game theory applications in humanitarian operations: A review. Journal of Humanitarian Logistics and Supply Chain Management 4(1), 4-23.

Nagurney, A., 1989. Migration equilibrium and variational inequalities. Economics Letters 31, 109-112.

Nagurney, A., 1990. A network model of migration equilibrium with movement costs. Mathematical and Computer Modelling 13, 79-88.

Nagurney, A., 1999. Network Economics: A Variational Inequality Approach, second and revised edition. Kluwer Academic Publishers, Dordrecht, The Netherlands.

Nagurney, A., Alvarez Flores, E., Soylu, C., 2016. A Generalized Nash Equilibrium model for post-disaster humanitarian relief. Transportation Research E 95, 1-18.

Nagurney, A., Besik, D., Dong, J., 2019. Tariffs and quotas in world trade: A unified variational inequality framework. European Journal of Operational Research 275(1), 347-360.

Nagurney, A., Daniele, P., 2020. International human migration networks under regulations. European Journal of Operational Research, in press.

Nagurney, A., Daniele, P., Flores, E.A., Caruso, V., 2017, July. A Variational Equilibrium Network Framework for Humanitarian Organizations in Disaster Relief: Effective Product Delivery Under Competition for Financial Funds. In International Conference on Dynamics

of Disasters, 109-133.

Nagurney, A., Dutta, P., 2019a. Competition for blood donations. Omega 85, 103-114.

Nagurney, A., Dutta, P., 2019b. Supply chain network competition among blood service organizations: a Generalized Nash Equilibrium framework. Annals of Operations Research 275(2), 551-586.

Nagurney, A., Pan, J., Zhao, L., 1992a. Human migration networks. European Journal of Operational Research 59, 262-274.

Nagurney, A., Pan, J., Zhao, L., 1992b. Human migration networks with class transformations. In Structure and Change in the Space Economy. Lakshmanan, T.R., Nijkamp, P., Editors, Springer-Verlag, Berlin, Germany, 239-258.

Nagurney, A., Salarpour, M., Daniele, P., 2019. An integrated financial and logistical game theory model for humanitarian organizations with purchasing costs, multiple freight service providers, and budget, capacity, and demand constraints. International Journal of Production Economics 212, 212-226.

Nagurney, A., Salarpour, M., Nagurney, L.S., 2020. A stochastic disaster relief game theory network model. SN Operations Research Forum 1, 10.

Nagurney, A., Zhang, D., 1996. Projected Dynamical Systems and Variational Inequalities with Applications. Kluwer Academic Publishers, Boston, Massachusetts.

New York Blood Center, 2020. Convalescent plasma- donor FAQ.
Available online: https://nybloodcenter.org/donate-blood/covid-19-and-blood-donation
-copy/convalescent-plasma-donor-faq/.

Osorio, A.F., Brailsford, S.C., Smith, H.K., Forero-Matiz, S.P., Camacho-Rodriguez, B.A., 2017. Simulation-optimization model for production planning in the blood supply chain. Health Care Management Science 20(4), 548-564.

Our World in Data, 2020. Total number of Covid-19 deaths. Available at:
https://ourworldindata.org/grapher/total-deaths-covid-19; retrieved on May 14, 2020.

Pan, J., Nagurney, A., 1994. Using Markov chains to model human migration in a network equilibrium framework. Mathematical and Computer Modelling 19, 31-39.

Pan, J., Nagurney, A., 2006. Evolution variational inequalities and projected dynamical

systems with application to human migration. Mathematical and Computer Modelling 43(5-6), 646-657.

Pawlowski, A., 2020. What is plasma? How to donate convalescent plasma for coronavirus patients. Today, April 23. Available online: https://www.today.com/health/what-plasma-donating-convalescent-covid-19-plasma-coronavirus-patients-t179700.

Piraban, A., Guerrero, W.J., Labadie, N., 2019. Survey on blood supply chain management: Models and methods. Computers and Operations Research 112, 104756.

Rassia, S.T., 2020. How architecture fails in conditions of crisis: a discussion on the value of interior design over the COVID-19 outbreak. SN Operations Research Forum 1, 13. Available online: https://doi.org/10.1007/s43069-020-0014-9.

Salehi, F., Mahootchi, M., Husseini, S.M.M., 2019. Developing a robust stochastic model for designing a blood supply chain network in a crisis: A possible earthquake in Tehran. Annals of Operations Research 283(1-2), 679-703.

Samani, M.R.G., Torabi, S.A., Hosseini-Motlagh, S.M., 2018. Integrated blood supply chain planning for disaster relief. International Journal of Disaster Risk Reduction 27, 168-188.

Saxton, G.D., Zhuang, J., 2013. A game-theoretic model of disclosuredonation interactions in the market for charitable contributions. Journal of Applied Communication Research 41(1), 40-63.

Schreiber, G.B., Schlumpf, K.S., Glynn, S.A., Wright, D.J., Tu, Y.L., King, M.R., Higgins, M.J., Kessler, D., Gilcher, R., Nass, C.C., Guiltinan, A.M., 2006. Convenience, the bane of our existence, and other barriers to donating. Transfusion 46, 545-553.

Schlumpf, K.S., Glynn, S.A., Schreiber, G.B., Wright, D.J., Randolph Steele, W., Tu, Y., Hermansen, S., Higgins, M.J., Garratty, G., Murphy, E., 2008. Factors influencing donor return. Transfusion 48(2), 264-272.

Shen, C., Wang, Z., Zhao, F., Yang, Y., Li, J., Yuan, J., Wang, F., Li, D., Yang, M., Xing, L., Wei, J., 2020. Treatment of 5 critically ill patients with COVID-19 with convalescent plasma. JAMA, 323(16), 1582-1589.

Sheridan, C. 2020. Convalescent serum lines up as first-choice treatment for coronavirus. May 7, Nature Biology. Available at: https://www.nature.com/articles/d41587-020-00011-1.

Toyasaki, F., Wakolbinger, T., 2014. Impacts of earmarked private donations for disaster fundraising. Annals of Operations Research 221(1), 427-447.

Van Griensven, J., Edwards, T., de Lamballerie, X., Semple, M.G., Gallian, P., Baize, S., Horby, P.W., Raoul, H., Magassouba, N.F., Antierens, A., Lomas, C., 2016. Evaluation of convalescent plasma for Ebola virus disease in Guinea. New England Journal of Medicine 374(1), 33-42.

Winkler, A.M., Koepsell, S.A., 2015. The use of convalescent plasma to treat emerging infectious diseases: focus on Ebola virus disease. Current Opinion in Hematology 22(6), 521-526.

Zhuang, J., Saxton, G.D., Wu, H., 2014. Publicity vs. impact in nonprofit disclosures and donor preferences: A sequential game with one nonprofit organization and N donors. Annals of Operations Research 221(1), 469-491.